International Journal of Microwave and Wireless Technologies

cambridge.org/mrf

A microstrip switched-band impedance transformer for frequency-dependent complex load

Ming-Lin Chuang, Ming-Tien Wu and Shu-Min Tsai

Department of Communication Engineering, National Penghu University of Science and Technology, Penghu, Taiwan

Research Paper

Cite this article: Chuang M-L, Wu M-T, Tsai S-M (2021). A microstrip switched-band impedance transformer for frequency-dependent complex load. *International Journal of Microwave and Wireless Technologies* **13**, 234–239. https://doi.org/10.1017/S1759078720001051

Received: 29 March 2020
Revised: 7 July 2020
Accepted: 8 July 2020
First published online: 3 August 2020

Key words:
Impedance transformer; switched-band; matching network

Author for correspondence:
Ming-Lin Chuang,
E-mail: morris@npu.edu.tw

Abstract

This study presents a simple switched-band impedance transformer using microstrip lines. The proposed circuit is suitable for loads with frequency-dependent complex impedances at two arbitrary operating frequencies. The transformer comprises two cascaded microstrip lines and two detachable shunt stepped-impedance stubs, which are separately connected to the main line via switching diodes such that provide good matching at one of the two operating frequencies and suppress unwanted signal at the other frequencies. The structure contains several user-set parameters such that designers can create a smaller circuit. The circuit parameters, except the user-set ones, are obtained using the derived design formula. The numerical simulations and experimental results agree well such that validate the proposed structure and the design formula.

Introduction

Impedance transformers or matching networks are important circuits in RF and microwave systems. In addition to providing good matching between two circuits, impedance transformers also affect the amplifier gain and noise figure of these systems. Impedance transformers consisting of transmission lines are commonly used because of the low cost and low parasitic effects owing to the absence of lumped elements or soldered connections.

As the demand for dual-band communication system increases, dual-band impedance transformers become more important. Dual-band impedance transformers using multi-section transmission lines have been developed to match a load with equal complex impedances [1] and frequency-dependent complex impedances [2]. Multi-section transmission lines with shunt stubs represent another configuration to match such loads [3–8]. Because shunt stubs can generate virtual ground, dual-band impedance transformers with a selectable transmission zero have been proposed to suppress unwanted out-of-band signals [9, 10]. Dual-band impedance transformer using two parallel transmission lines has also been developed [11].

Most of these studies have focused on concurrently achieving matching at the two operating frequencies. However, modern dual-band communication systems often operate at only one of these two frequencies. For instance, commercial WiFi equipment connects to an access point via either the 2.4 or 5.8 GHz band at an instant. Once an operating frequency is selected, the other one is often turned off to save power and avoid problems. The amplifier used in such cases generally combines two individual amplifiers with switches [12]. However, this topology requires a large circuit area and more components. Another way of implementing such an amplifier involves a single transistor with switchable input and output impedance transformers. One possible way uses switchable inductor and capacitor as an output matching network [13]. Another way of this type of switchable amplifier uses cascaded transmission lines and detachable shunt uniform stubs [14–16]. A switched band impedance transformer with a detached shunt stub and a fixed shunt stub has also been proposed [17]. The common limitation in these works is that the characteristic impedances of the cascaded transmission lines must be 50 Ω, which restrict the design freedom and the circuit size is fixed. Further, these circuits provide good matching at the operating frequency, but do not guarantee total reflection at the non-operating frequency. Therefore, such systems may generate a large RF signal at the operating frequency and a non-negligible RF signal that is only slightly smaller at the non-operating frequency.

This work presents a switched-band impedance transformer composed of two cascaded transmission lines and two detachable shunt stepped-impedance open stubs with switching diodes to control the operating mode. With this transformer, the two aforementioned limitations of the previous works are resolved. The circuit parameters are obtained using the derived analytical design formula. Numerical simulations and experimental measurements are presented to validate the proposed structure and design formula.

© Cambridge University Press and the European Microwave Association 2020

CAMBRIDGE UNIVERSITY PRESS

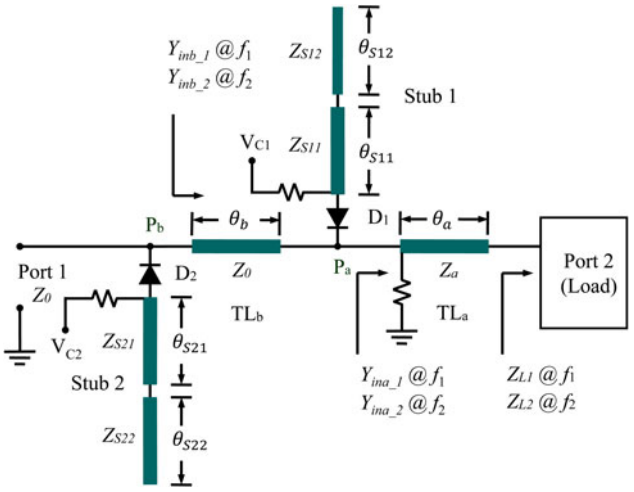


Fig. 1. The proposed switched band impedance transformer.

Transformer structure and design formula

This work considers two operating frequencies, f_1 and f_2, which are arbitrary and uncorrelated. The frequency ratio is defined as $\alpha \equiv f_2/f_1$. The load is considered to have a frequency-dependent complex impedance, i.e. the load impedances at the two operating frequencies are different. Figure 1 shows the structure of the proposed switched band impedance transformer. The electrical lengths of the transmission lines and stubs are measured at frequency f_1.

If transmission line TL_a and stub 1 are used to match the lower frequency, f_1, the functions of the transmission lines and stubs as well as the design concept are described below. Transmission line TL_a is used to obtain an input admittance Y_{ina_1}, seen by looking into the load and having the form $Y_0 + jB_{ina_1}$ at frequency f_1. If the load impedances at the two operating frequencies are $Z_{L1} = R_{L1} + jX_{L1}$ at f_1 and $Z_{L2} = R_{L2} + jX_{L2}$ at f_2, the electric length, θ_a, of transmission line TL_a can be determined as

$$\theta_a = \tan^{-1}\left(\frac{Z_a X_{L1} \pm \sqrt{Z_a^2 X_{L1}^2 - (Z_a^2 - Z_0 R_{L1})(|Z_{L1}|^2 - Z_0 R_{L1})}}{Z_0 R_{L1} - Z_a^2}\right), \tag{1}$$

where the characteristic impedance Z_a is a user-set parameter. Comparing with the previous study [17], Z_a can be an arbitrary value instead of Z_0.

Once the input admittance is calculated, a shunt stub is added to cancel the input susceptance. When diode D_1 is forward biased and diode D_2 is reverse biased, stub 1 is connected to transmission line TL_a at junction P_a and stub 2 is disconnected. Uniform-impedance stub[14] can be used to cancel the input susceptance at f_1 but not guarantee to block the signal at f_2. In this study, stub 1, which has a stepped impedance, is used to cancel input susceptance B_{ina_1} at f_1 and generate a transmission zero (total reflection), to block the signal at f_2. Therefore, the lengths and the characteristic impedance of stub 1 must meet equations (2) and (3).

$$\frac{1}{Z_{S11}} \frac{Z_{S11} + Z_{S12}\cot(\theta_{S12})\tan(\theta_{S11})}{Z_{S11}\tan(\theta_{S11}) - Z_{S12}\cot(\theta_{S12})} = -B_{ina_1}, \tag{2}$$

$$Z_{S11} \frac{Z_{S11}\tan(\alpha\theta_{S11}) - Z_{S12}\cot(\alpha\theta_{S12})}{Z_{S11} + Z_{S12}\cot(\alpha\theta_{S12})\tan(\alpha\theta_{S11})} = 0. \tag{3}$$

Solving these simultaneous equations for Z_{S11} and Z_{S12} yields

$$Z_{S11} = \frac{1}{B_{ina_1}} \frac{1 + \tan(\theta_{S11})\cot(\theta_{S12})\tan(\alpha\theta_{S11})\tan(\alpha\theta_{S12})}{\tan(\theta_{S11}) - \cot(\theta_{S12})\tan(\alpha\theta_{S11})\tan(\alpha\theta_{S12})}, \tag{4}$$

$$Z_{S12} = Z_{S11}\tan(\theta_{S11})\tan(\alpha\theta_{S12}), \tag{5}$$

where the electrical lengths θ_{S11} and θ_{S12} are user-set parameters. Thus, the load impedance is transformed to Z_0 at f_1 and short-circuited at f_2.

To achieve matching at frequency f_2, diode D_1 is reverse biased and D_2 is forward biased. Thus, stub 1 is disconnected and stub 2 is connected to transmission line TL_b at junction P_b. Transmission lines TL_a and TL_b are used to obtain the input admittance Y_{inb_2}, at junction P_b, seen by looking into the load and have the form $Y_0 + jB_{inb_2}$ at frequency f_2. The characteristic impedance of transmission line TL_b is chosen as Z_0 so that it does not affect the matching condition at f_1.

The electrical length, θ_b, of transmission line TL_b at frequency f_1 can be determined as

$$\theta_b = \frac{1}{\alpha}\tan^{-1}\left(\frac{X_{ina_2} \pm \sqrt{R_{ina_2}[(Z_0 - R_{ina_2})^2 + X_{ina_2}^2]/Z_0}}{R_{ina_2} - Z_0}\right), \tag{6}$$

where the input impedance at junction P_a without stub 1 is $R_{ina_2} + jX_{ina_2}$ at frequency f_2.

Once the input conductance is obtained, stub 2 is used to cancel input susceptance B_{inb_2} at f_2 and generate a virtual ground to block the signal at f_1. Therefore, the lengths and the characteristic impedance of stub 2 must satisfy equations (7) and (8) simultaneously.

$$Z_{S21} \frac{Z_{S21}\tan(\theta_{S21}) - Z_{S22}\cot(\theta_{S22})}{Z_{S21} + Z_{S22}\cot(\theta_{S22})\tan(\theta_{S21})} = 0\,, \tag{7}$$

$$\frac{1}{Z_{S21}} \frac{Z_{S21} + Z_{S22}\cot(\alpha\theta_{S22})\tan(\alpha\theta_{S21})}{Z_{S21}\tan(\alpha\theta_{S21}) - Z_{S22}\cot(\alpha\theta_{S22})} = -B_{inb_2}. \tag{8}$$

Solving these equations for Z_{S21} and Z_{S22} yields

$$Z_{S21} = \frac{1}{B_{inb_2}} \frac{1 + \tan(\theta_{S21})\cot(\theta_{S22})\tan(\alpha\theta_{S21})\tan(\alpha\theta_{S22})}{\tan(\theta_{S21}) - \cot(\theta_{S22})\tan(\alpha\theta_{S21})\tan(\alpha\theta_{S22})}, \tag{9}$$

$$Z_{S22} = Z_{S21}\tan(\theta_{S21})\tan(\theta_{S22}), \tag{10}$$

where the electrical lengths θ_{S21} and θ_{S22} are user-set parameters. Thus, the load impedance is transformed to Z_0 at f_2 and short-circuited at f_1. For convenience, the above solution is called Type 1.

https://doi.org/10.1017/S1759078720001051 Published online by Cambridge University Press

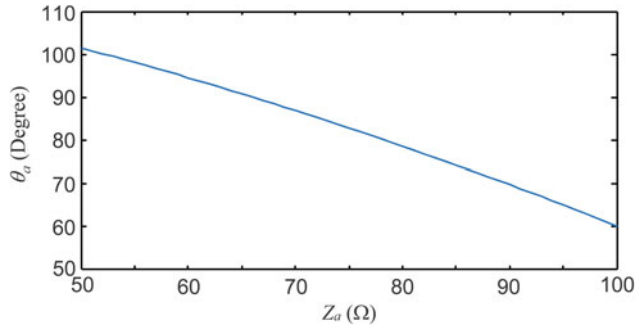


Fig. 2. Variation of the required electrical length θ_a (at 0.9 GHz) versus the characteristic impedance Z_a of transmission line TL_a for Type 1.

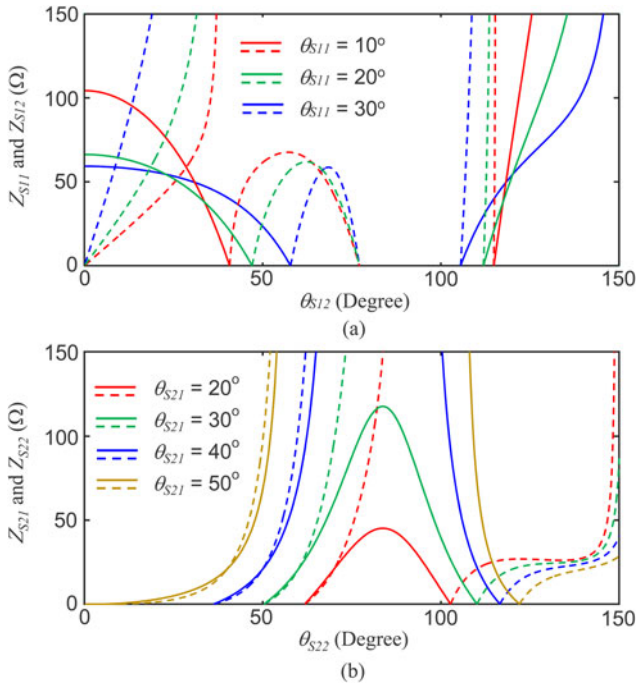


Fig. 3. Variation of the required stub impedances versus stub lengths, (a) Z_{S11} (solid line) and Z_{S12} (dashed line) against θ_{S12} for different θ_{S11}, (b) Z_{S21} (solid line) and Z_{S22} (dashed line) against θ_{S22} for different θ_{S21}.

The functions of the transmission lines and stubs can be interchanged with the same circuit structure. For convenience, this solution is called Type 2. Specifically, transmission line TL_a and stub 1 in Type 1 are used to match the lower frequency, f_1, while transmission line TL_a and stub 1 in Type 2 are used to match the higher frequency, f_2.

In Type 2, transmission line TL_a is used to obtain an input admittance seen by looking into the load and having unit conductance at frequency f_2 while stub 1 is used to cancel the susceptance arising from transmission line TL_a at frequency f_2 and to generate a transmission zero at frequency f_1 when diode D_1 is forward biased and diode D_2 is reverse biased. For matching at frequency f_1, diode D_1 is reverse biased and D_2 is forward biased. Thus, stub 1 is disconnected and stub 2 is connected to transmission line TL_b. Transmission lines TL_a and TL_b are used to obtain a certain input admittance so as to have unit admittance at frequency f_1. Stub 2 is used to cancel the susceptance arising from transmission lines TL_a and TL_b at frequency f_1 and to generate

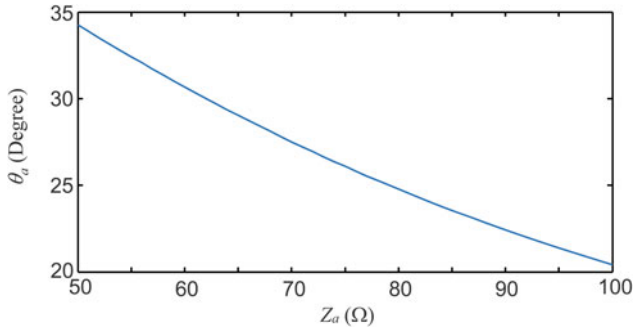


Fig. 4. Variation of the required electrical length θ_a (at 0.9 GHz) versus the characteristic impedance Z_a of transmission line TL_a for Type 2.

a transmission zero (total reflection), at frequency f_2. In this case, the design formula is modified as equations (11)–(16).

$$\theta_a = \frac{1}{\alpha}\tan^{-1}\left(\frac{Z_a X_{L2} \pm \sqrt{Z_a^2 X_{L2}^2 - (Z_a^2 - Z_0 R_{L2})(|Z_{L2}|^2 - Z_0 R_{L2})}}{Z_0 R_{L2} - Z_a^2}\right), \tag{11}$$

$$Z_{S11} = \frac{1}{B_{ina_2}}\frac{1 + \tan(\theta_{S11})\tan(\theta_{S12})\tan(\alpha\theta_{S11})\tan(\alpha\theta_{S12})}{\tan(\alpha\theta_{S11}) - \tan(\theta_{S11})\tan(\theta_{S12})\cot(\alpha\theta_{S12})}, \tag{12}$$

$$Z_{S12} = Z_{S11}\tan(\theta_{S11})\tan(\theta_{S12}), \tag{13}$$

and

$$\theta_b = \tan^{-1}\left(\frac{X_{ina_1} \pm \sqrt{R_{ina_1}[(Z_0 - R_{ina_1})^2 + X_{ina_1}^2]/Z_0}}{R_{ina_1} - Z_0}\right), \tag{14}$$

$$Z_{S21} = \frac{1}{B_{inb_1}}\frac{1 + \tan(\theta_{S21})\cot(\theta_{S22})\tan(\alpha\theta_{S21})\tan(\alpha\theta_{S22})}{\tan(\theta_{S21}) - \cot(\theta_{S22})\tan(\alpha\theta_{S21})\tan(\alpha\theta_{S22})}, \tag{15}$$

$$Z_{S22} = Z_{S21}\tan(\alpha\theta_{S21})\tan(\alpha\theta_{S22}). \tag{16}$$

In these equations, B_{ina_2} denotes the input susceptance at frequency f_2 at junction P_a, $R_{ina_1} + jX_{ina_1}$ denotes the input impedance at frequency f_1 at junction P_a without stub 1, and B_{inb_1} denotes the input susceptance at frequency f_1 at junction P_b.

Design example

To verify the proposed structure and design procedure, a switched band impedance transformer using microstrips was designed, fabricated, and measured. The arbitrary two operating frequencies used were 0.9 and 2.1 GHz. The transformer was designed and fabricated on a 1.6 mm-thick FR4 substrate with a dielectric constant of 4.35 and a loss tangent of 0.016. The load used was a 100 Ω resistor and an SMA connector shunt connected with a 1 pF

https://doi.org/10.1017/S1759078720001051 Published online by Cambridge University Press

Table 1. Circuit parameters of the designed switched band impedance transformers where parameters with underline are user-setting.

	Z_a (Ω)	Z_b (Ω)	Z_{S11} (Ω)	Z_{S12} (Ω)	Z_{S21} (Ω)	Z_{S22} (Ω)
Type 1	75.00	50.00	70.28	49.15	51.08	67.61
Type 2	75.00	50.00	45.67	39.36	57.35	75.90
	θ_a (°)	θ_b (°)	θ_{S11} (°)	θ_{S12} (°)	θ_{S21} (°)	θ_{S22} (°)
Type 1	82.80	29.32	10.00	25.00	50.00	48.00
Type 2	26.09	84.94	15.00	20.00	50.00	48.00

The electrical lengths are measured at 0.9 GHz.

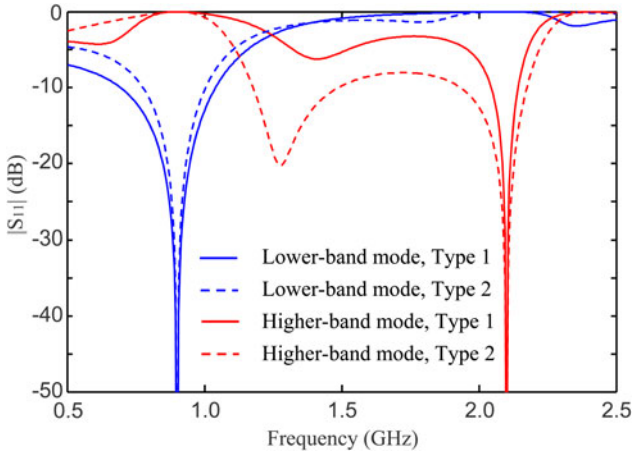


Fig. 5. Simulated reflection coefficients of the two designed switch-band impedance transformers with different diode biasing conditions.

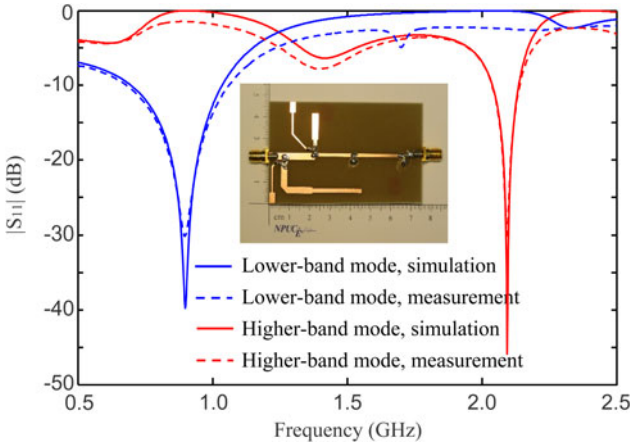


Fig. 7. Simulated and measured reflection coefficients of the fabricated switched band impedance transformer with different diode biasing conditions.

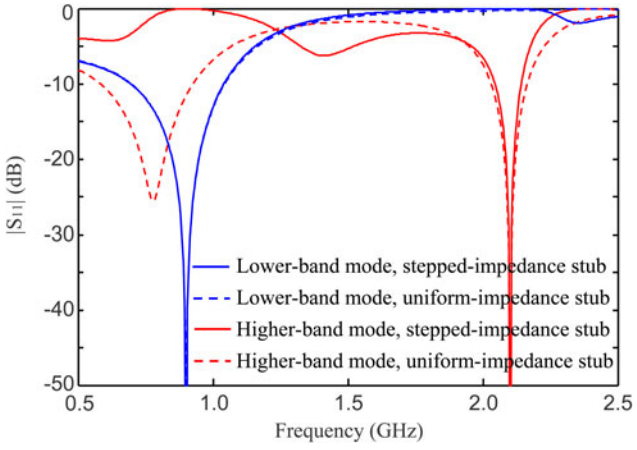


Fig. 6. Comparison between impedance transformers with uniform-impedance stubs and stepped-impedance stubs.

capacitor. The corresponding load impedances were 87.24-j74.00 and 30.50-j60.38 Ω at the two operating frequencies, respectively.

Figure 2 shows the variation of the required electrical length θ_a versus the characteristic impedance Z_a of transmission line TL_a for Type 1. In this case, the length θ_a decreases as the impedance Z_a increases. Because Z_a is a user-set parameter, the designer can choose a suitable value to minimize θ_a under PCB fabrication constrains, such as width limitations. In contrast, traditional single-frequency matching networks or previous switched matching networks[14] often use a 50 Ω transmission line, such that the circuit size is fixed and cannot be reduced. For example, the required length θ_a is about 60° if Z_a was chosen as 100 Ω which is a typical upper value of general PCB technique. While if Z_a was chosen to be equal to the traditional value of 50 Ω, the required length θ_a would be more than 100°. The proposed structure can reduce the required length by 60%. In this example, Z_a was chosen as 75 Ω and the required θ_a was 82.80° at 0.9 GHz.

As to transmission line TL_b, there were two solutions that could be chosen. In this example, θ_b was chosen as 29.32° at 0.9 GHz. Figure 3(a) demonstrates the variations of the required Z_{S11} and Z_{S12} versus θ_{S12} for different values of θ_{S11}. Because θ_{S12} and θ_{S11} are user-set parameters, suitable values can be chosen to obtain reasonable stub impedances, i.e. neither extremely high nor extremely low. For example, Z_{S11} and Z_{S12} are between 25 and 100 Ω when $\theta_{S11} = 10°$ and $13° < \theta_{S12} < 35°$. Figure 3(b) shows a similar phenomenon for stub 2.

For Type 2, Fig. 4 demonstrates the variation of the required electrical length θ_a versus the characteristic impedance Z_a of transmission line TL_a. Figure 4 shows that a higher impedance transmission line requires a shorter length. As Type 1, the designer can choose a suitable value to minimize θ_a under PCB fabrication constrain, such as width limitations. Here Z_a was chosen to be 75 Ω as Type 1 and thus the required length θ_a was 26.09° at 0.9 GHz. In contrast, the switched matching network that uses a 50 Ω transmission line requires θ_a of more than 34°. The choice of the characteristic impedances and lengths of stubs 1 and 2 is similar to Type 1.

https://doi.org/10.1017/S1759078720001051 Published online by Cambridge University Press

Table 2. Comparison between this work and other researches

	Design method	Suppression of non-operating band	Microstrip impedance	Circuit area
[14]	Analytical	No	Fixed (50 Ω)	Fixed
[15]	Analytical	No	Fixed (50 Ω)	Fixed
[17]	Analytical	No	Fixed (50 Ω)	Fixed
This work	Analytical	Yes	Arbitrary	Reducible

Table 1 lists the parameters of the two designed circuits, where the underlined values denote user-set parameters and the rest were obtained using the proposed design formula. Figure 5 shows the frequency responses of the two designed switchable transformers which were simulated using Ansoft Designer (now called ANSYS HFSS-Circuit) with ideal transmission line model. The diodes were considered as ideal in our numerical simulation, i.e. open when zero-biased and shorted when forward-biased. In the lower-band mode, diode D_1 is forward-biased and diode D_2 is zero-biased. In this mode, the frequency response showed a good matching exactly at the operating frequency, 0.9 GHz, and a reflection of 0 dB at the non-operating frequency, 2.1 GHz. In the higher-band mode, diode D_1 is zero-biased and diode D_2 is forward-biased. The frequency response showed a good matching exactly at 2.1 GHz and a reflection of 0 dB at 0.9 GHz. Due to the restriction of total reflection at the non-operating frequency, the matching bandwidth of the presented impedance transformer is narrower than the traditional single-band impedance transformer which does not concern with total reflection at other frequencies.

Figure 6 compares the numerical results of Type 1 using stepped-impedance stubs and traditional structure using uniform-impedance stubs. If the matching frequency is 2.1 GHz, the structure using stepped-impedance has S_{11} of 0 dB at 0.9 GHz while the structure using uniform-impedance stub has S_{11} of −12 dB. It is clear that the circuit using stepped-impedance stub can suppress signal at the non-operating frequency and the one using uniform-impedance stub has no such function.

Figure 7 shows a comparison of the numerical and measured frequency responses where the fabricated transformer Type 1 is embedded. This work used Infineon BAR63-02V PIN diodes. The experimental results were obtained using an R&S ZVA40 network analyzer. In the lower-band mode, the simulation revealed a good match at 0.9 GHz and total reflection (0 dB) at 2.1 GHz. The measurements showed good matching at 0.9 GHz and a reflection of −2.4 dB at 2.1 GHz. The bandwidths of the simulations and measurement are 338 and 383 MHz, respectively. In the higher-band mode, the simulation revealed a good match at 2.1 GHz and total reflection at 0.9 GHz. The bandwidths of the simulations and measurement are 98 and 113 MHz, respectively. The measurements showed a good match at 2.1 GHz and a reflection of −1.4 dB at 0.9 GHz. The deviations between the simulated and measured results may be due to fabrication errors, discontinuity effects, substrate losses, and non-ideal diodes. These factors were not considered in the design formula and simulation. The non-zero forward resistance of the PIN diode in the ON state, which degrades the virtual ground at junctions P_a and P_b, can be improved by replacing the PIN diode with an MEM switch, which has a very low insertion loss in the ON state, may improve the measured reflection at the non-operating frequency.

Table 2 compares this work and published researches about switched-band impedance transformers.

Conclusion

This work presents a switched-band matching network that can match a frequency-dependent complex impedance load at one of the two uncorrelated frequencies. The characteristic impedance of the transmission line connected to the load can be arbitrary instead of the traditional Z_0, which can potentially reduce the size of the circuit. The detachable stepped-impedance shunt stubs ensure good matching at one of the two frequencies and a virtual ground that suppresses the signal at the non-operating frequency. The derived analytical formula simplifies the design process and does not involve time-consuming iterative procedures. The numerical simulations and experimental measurements validated the proposed structure and design formula. The presented structure can thus be applied to switched-band amplifier and mixer designs.

References

1. **Wu Y, Liu Y and Li S** (2009) A dual-frequency transformer for complex impedances with two unequal sections. *IEEE Microwave and Wireless Components Letters* **2**, 77–79.
2. **Liu X, Liu Y, Li S, Wu F and Wu Y** (2009) A three-section dual-band transformer for frequency-dependent complex load impedance. *IEEE Microwave and Wireless Components Letters* **10**, 611–613.
3. **Rawat K and Ghannouchi FM** (2011) Dual-band matching technique based on dual-characteristic impedance transformers for dual-band power amplifiers design. *IET Microwave Transactions on Antennas and Propagation* **14**, 1720–1729.
4. **Fu X, Bespalko DT and Boumaiza S** (2012) Novel dual-band matching network topology and its application for the design of dual-band class J power amplifiers. *2012 IEEE MTT-S Microwave Symposium Digest, Montreal, Canada, June 2012.*
5. **Fu X, Bespalko D and Boumaiza S** (2014) Novel dual-band matching network for effective design of concurrent dual-band power amplifiers. *IEEE Transactions on Circuits and Systems I* **1**, 293–301.
6. **Manoochehri O, Asoodeh A and Forooraghi K** (2015) PI-model dual-band impedance transformer for unequal complex impedance loads. *IEEE Microwave and Wireless Components Letters* **4**, 238–240.
7. **Maktoomi MA, Panwar V, Hashmi MS and Ghannouchi FM** (2016) Improving load range of dual-band impedance matching networks using novel load-healing concept. *IEEE Transactions on Circuits and Systems II* **2**, 126–130.
8. **Liu J, Zhang XY and Yang C-L** (2018) Analysis and design of dual-band rectifier using novel matching network. *IEEE Transactions on Circuits and System II* **3**, 431–435.
9. **Chuang M-L and Wu M-T** (2016) General dual-band impedance transformer with a selectable transmission zero. *IEEE Transactions on Components Packaging and Manufacturing Technology* **7**, 1113–1119.
10. **Chuang M-L and M-T Wu** (2017) Transmission zero embedded dual-band impedance transformer with three shunt stubs. *IEEE Microwave and Wireless Components Letters* **9**, 788–790.
11. **Wang X, Ma Z and Ohira M** (2017) Dual-band design theory for dual transmission-line transformer. *IEEE Microwave and Wireless Components Letters* **9**, 782–784.

https://doi.org/10.1017/S1759078720001051 Published online by Cambridge University Press

12. **Candra P and Xia T** (2016) SiGe HBT X-band and Ka-band switchable dual-band low noise amplifier. *IEEE International Symposium on Circuits and Systems, Montréal, QC, Canada, May 2016*.
13. **Ko J, Lee S and An SN** (2017) S/X-Band CMOS power amplifier using a transformer-based reconfigurable output matching network. *IEEE International Symposium on Radio Frequency Integrated Circuits, Honolulu, HI, USA, July 2017*.
14. **Fukuda A, Okazaki H, Hirota T and Yamao Y** (2004) Novel 900 MHz/1.9 GHz dual-mode power amplifier employing MEMS switches for optimum matching. *IEEE Microwave and Wireless Components Letters* **3**, 121–123.
15. **Fukuda A, Okazaki H, Narahashi S, Hirota T and Yamao Y** (2005) A 900/1500/2000–MHz triple-band reconfigurable power amplifier employing RF-MEM switches. *2005 IEEE MTT-S Microwave Symposium Digest, Long Beach, CA, USA, June 2005*.
16. **Norouzian F** (2015) *Dual-Band and Switched-Band Highly Efficient Power Amplifiers*. (Ph.D. Thesis), University of Birmingham, UK.
17. **Norouzian F and Gardner P** (2012) Analytical solution for switched band matching networks. *3rd Annual Seminar on Passive RF and Microwave Components, London, UK, March 2012*.



Ming-Lin Chuang received the B.S. degree in electrical engineering from National Central University, Taoyuan, Taiwan, in 1991, M.S. and Ph.D. degrees in electrical engineering from Tatung Institute of Technology, Taipei, Taiwan, in 1993 and 1998, respectively. In 2000, he joined the faculty of the Department of Communication Engineering, National Penghu University of Science and Technology, Penghu, Taiwan, and as the chair from 2000 to 2005 and 2010 to 2016. He is currently the Professor of the department. Dr. Chuang's research interests include RF/microwave passive and active circuits, antennas, and Internet of things.



Ming-Tien Wu received the B.S. and Ph.D. degrees in electrical engineering from Tatung Institute of Technology, Taipei, Taiwan, in 1988 and 1996, respectively. In 1998, he joined the faculty of the Department of Communication Engineering, National Penghu University of Science and Technology, Penghu, Taiwan. He is currently the Associate Professor and Chair of the department. Dr. Wu's areas of research include microwave passive circuits and antennas.



Shu-Min Tsai received the B.S. degree from the National Taiwan Ocean University, Keelung, Taiwan, in 1992, and the M.S. degree in 1994, respectively, and the Ph.D. degree from the National Cheng Kung University, Tainan, Taiwan, in 2007, all in Electrical Engineering department. She is now an Associate Professor in the Department of Communication Engineering of National Penghu University of Science and Technology, Penghu, Taiwan. Dr. Tsai's research interests include communication circuit and system, Internet of things, and signal processing.

https://doi.org/10.1017/S1759078720001051 Published online by Cambridge University Press